JMB

The Mechanical Hierarchies of Fibronectin Observed with Single-molecule AFM

Andres F. Oberhauser*, Carmelu Badilla-Fernandez Mariano Carrion-Vazquez and Julio M. Fernandez*

Department of Physiology and Biophysics, Mayo Foundation Rochester, MN 55905, USA

Mechanically induced conformational changes in proteins such as fibronectin are thought to regulate the assembly of the extracellular matrix and underlie its elasticity and extensibility. Fibronectin contains a region of tandem repeats of up to 15 type III domains that play critical roles in cell binding and self-assembly. Here, we use single-molecule force spectroscopy to examine the mechanical properties of fibronectin (FN) and its individual FNIII domains. We found that fibronectin is highly extensible due to the unfolding of its FNIII domains. We found that the native FNIII region displays strong mechanical unfolding hierarchies requiring 80 pN of force to unfold the weakest domain and 200 pN for the most stable domain. In an effort to determine the identity of the weakest/strongest domain, we engineered polyproteins composed of an individual domain and measured their mechanical stability by single-protein atomic force microscopy (AFM) techniques. In contrast to chemical and thermal measurements of stability, we found that the tenth FNIII domain is mechanically the weakest and that the first and second FNIII domains are the strongest. Moreover, we found that the first FNIII domain can acquire multiple, partially folded conformations, and that their incidence is modulated strongly by its neighbor FNIII domain. The mechanical hierarchies of fibronectin demonstrated here may be important for the activation of fibrillogenesis and matrix assembly.

© 2002 Elsevier Science Ltd. All rights reserved

Keywords: fibronectin; hierarchies; mechanical unfolding; AFM; single molecule

*Corresponding authors

Introduction

The extracellular matrix (ECM) determines the elasticity and tensile strength of tissues, and regulates cell adhesion and cell migration finely. The intact ECM is under a constantly changing mechanical stress. Fibronectin (FN) is an important component of the ECM. Mechanical stretching of fibronectin is thought to be a physiological signal that triggers matrix assembly.[1–5] Fibronectin is composed of tandem repeats of three distinct types (I, II and III) of individually folded modules. Fibronectin type III modules (FNIII) contain binding sites for several membrane receptors and ECM components that play a role in the assembly of the ECM. For example, it is now well established that some of the critical interactions are the binding of [10]FNIII to integrins; the binding of [1]FNIII to other fibronectin molecules and the binding of [12–14]FNIII to heparin, another major component of the extracellular matrix.[4–7]

Although it is well accepted that mechanical tension is an important physiological signal in matrix assembly and function, it is not known how the fibronectin protein transduces the mechanical force into a physiological signal. However, there are some very appealing hypotheses: the most developed proposes that there are binding sites hidden in the folded core of FNIII modules and that upon a mechanical stretch, these modules unfold and become "activated". Exposure of these cryptic sites by mechanical unfolding triggers the binding of FNIII modules from other molecules, causing matrix assembly.[4,8–10] There are several putative cryptic binding sites in fibronectin: [1]FNIII, [2]FNIII, [1]FNIII, [10]FNIII.[4,8–10] Zhong *et al.* showed that a monoclonal antibody that binds
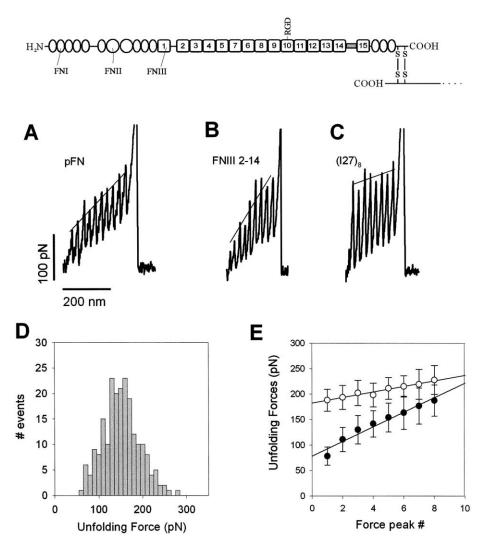
Figure 1. Mechanical hierarchies of native fibronectin captured by single-molecule force spectroscopy. The inset at the top shows a diagram of the modular structure of fibronectin. (a) Example of a force–extension curve of native bovine fibronectin, pFN. (b) Example of a force–extension curve of a recombinant fibronectin protein containing FNIII domains 2–14. (c) Sawtooth pattern obtained from a polyprotein containing identical repeats of the titin I27 domain. (d) Frequency histogram of unfolding forces for native fibronectin ($n = 197$ force-peaks). (e) Relationship between the unfolding force and the force-peak position in the sawtooth patterns obtained from native fibronectin (filled circles; $n = 6$ recordings) and an $(I27)_8$ polyprotein (open circles; $n = 46$ recordings). The slopes of the continuous lines correspond to an increase of 5.5 pN/peak for the $(I27)_8$ polyprotein and 16.2 pN/peak for native fibronectin. These values were obtained at a fixed pulling speed (0.6 μm/s).

[1]FNIII and blocks matrix assembly showed increased binding if the fibronectin matrix was stretched mechanically.[4] These experiments showed that the antibody binds a cryptic site in [1]FNIII that is exposed by the mechanical stretching of fibronectin. However, there is evidence that [1]FNIII does not act alone, and that [2]FNIII possesses a binding site that plays a fundamental role in fibrillogenesis.[10] What is now clear is that fibrillogenesis of fibronectin requires a mechanically activated form of the [1–2]FNIII modules. It is logical then to conclude that these modules would be mechanically weak, allowing them to respond easily to a stretching force.

Initial attempts to determine the stability of fibronectin have made use of thermal, chemical and even computational techniques.[11–18] In these experiments, either single modules or proteolytic fragments of the FNIII region were probed with scanning calorimetry to determine the temperatures at which the individual modules unfolded. For example, it was found that [10]FNIII is significantly more thermostable than [1]FNIII. These studies revealed a wide range of melting temperatures following the order [3]FNIII (121 °C) > [6]FNIII (111 °C) > [10]FNIII (102 °C) > [7]FNIII (95 °C) > [1]FNIII (78 °C) > [2]FNIII (57 °C) = [4]FNIII = [5]FNIII = [8]FNIII = [9]FNIII > [11]FNIII (48 °C).[11] The [10]FNIII region contains the integrin binding site defined by the RGD sequence. Deformation of this module by a mechanical force is predicted to affect the binding affinity for integrins greatly,[17] hence, if

[10]FNIII is very stable one might predict that the binding of an integrin under a stretching force will not alter the binding site. In contrast, [1]FNIII was found to be considerably more thermolabile and again that fits with the observation that the [1]FNIII module exists in a partially unfolded form that is ready to promote the self-assembly of a fibronectin matrix at a low stretching force.[8,9]

Through the use of novel single-molecule force spectroscopy techniques, it has been possible to study the mechanical stability of a wide variety of proteins.[19–32] With this technique, it has been possible to compare the thermodynamic and mechanical stability of immunoglobulin modules.[33] These experiments showed that thermodynamic stability could not predict the mechanical stability of these protein modules.[33] Similarly, we anticipated that the thermostability hierarchies determined by calorimetry would be poor predictors of the mechanical hierarchies of the fibronectin molecules. Since the fibronectin modules unfold driven by a stretching force rather than thermal or chemical changes, it is important to measure directly the mechanical unfolding hierarchies of fibronectin, if they exist.

In this work, we use protein engineering and single-molecule force spectroscopy to examine the mechanical design of the type III region of fibronectin.

Results

The native FNIII region of fibronectin displays strong mechanical unfolding hierarchies

In order to measure the mechanical properties of single fibronectin molecules, we used an AFM instrument designed specifically to study the mechanics of single proteins with great precision and high resolution.[29] In a typical experiment, the protein sample is placed on a gold-coated coverslip that is attached to the piezoelectric positioner. Single fibronectin proteins are then picked up randomly by adsorption to the AFM tip and stretched for up to several hundred nanometers. Stretching native fibronectin results in sawtooth patterns with force-peaks (Figure 1(a)) that had a mean value of 145 pN (Figure 1(d)). These results are similar to those of the AFM experiments on native fibronectin reported by Rief *et al.*[22] and Oberdorfer *et al.*[26] The increase in contour length was ∼28.5 nm, a distance that is consistent with the length of an unfolded FNIII domain (∼90 amino acid residues). Although there are 14 FNI and FNII domains these are much shorter, with 45 and 60 residues, respectively, and contain internal disulfide bonds that are likely to prevent their unfolding and hence do not contribute to the force-peaks in the sawtooth pattern. Indeed, a recombinant fibronectin protein containing FNIII domains 2–14 gave similar results (Figure 1(b)), demonstrating that the sawtooth pattern corresponds to the sequential unfolding of individual FNIII domains.

A characteristic feature of these traces is the continuous increase in the force required to unfold the individual FNIII modules, from about 80 to 200 pN (lines in Figure 1(a) and (b)). Figure 1(e) (filled circles) shows that the height of the force-peak correlates with its position in the sawtooth pattern for native fibronectin; early force-peaks show an unfolding force that is about half that of the force-peaks that occur later in the sawtooth pattern. The continuous line is a linear fit to the data obtained for native fibronectin (filled circles) and the slope corresponds to an increase of 16.2 pN/peak. Previous theoretical studies on the unfolding behavior of identical domains linked in series predict that the resulting sawtooth patterns should show a hierarchical relationship.[34,35] To test this prediction, we measured the unfolding forces for a protein containing identical repeats of the titin I27 domain,[24] and plotted the height of each individual force-peak as a function of its position in the sawtooth pattern (Figure 1(e), open circles). The data show that there is a slight tendency for early force-peaks to have smaller unfolding forces where the last peak is about 20% (30 pN) higher in force than the first (with a slope of 5.5 pN/peak). This apparent hierarchy may result from the decrease in unfolding probability, as more domains are unfolded. It is clear, however, that this effect cannot explain the pronounced slope in fibronectin, where we observed a difference of about 250% (120 pN) between the force of the last and first peak in the sawtooth patterns.

Thus, the native FNIII region of fibronectin displays strong mechanical unfolding hierarchies requiring 80 pN of force to unfold the weakest module and 200 pN for the most stable module.

Design of FNIII polyproteins

In order to understand the molecular basis of the unfolding hierarchy, we examined the mechanical properties of individual FNIII modules. For this, we constructed polyproteins containing tandem repeats of different fibronectin FNIII domains. We were able to clone and express eight different polyproteins containing FNIII domains 1, 2, 10, 12 and 13 (see Materials and Methods). We attempted to make polyproteins for other FNIII domains like [7]FNIII, [8]FNIII, [9]FNIII, or from dimers like [7]FNIII–[8]FNIII and [9]FNIII–[10]FNIII but encountered difficulties with the expression of these constructs, making them unsuitable for AFM studies. We selected the boundaries for FNIII domains 10, 12, 13 from the crystal structures of these domains (see Materials and Methods).[7,36] Given the absence of a structure for the [1]FNIII module, we had to guess its boundaries. This was important, because the boundaries are known to affect the stability of a protein.[37] To do this, we constructed four [1]FNIII polyproteins based on different boundaries (see Materials and Methods). The shortest [1]FNIII
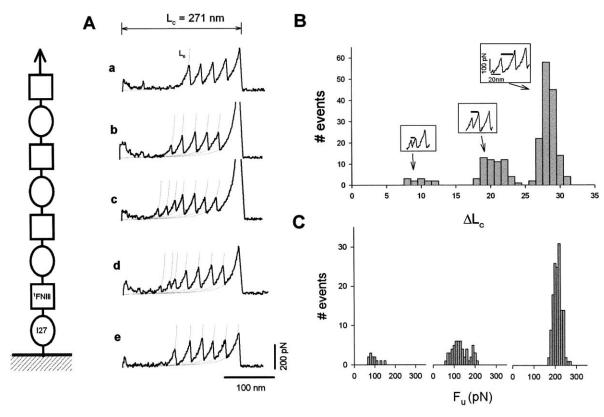
Figure 2. The "classic" ^{1}FNIII domain displays low mechanical stability and partially folded intermediates. (a) (a–e) Force–extension relationships for an $(I27-{}^1FNIII)_4$ polyprotein. The thin lines are fits of the WLC model to the data. Notice that all these recordings have about the same length, starting form the point where the cantilever is in contact with the coverslip to the last force-peak (which correspond to the detachment of the protein from the cantilever). The contour length of the fully stretched $(I27-{}^1FNIII)_4$ polyprotein was about 280 nm ($283(\pm 11)$ nm, $n = 22$), a value that is similar to the expected contour length of an unfolded $(I27-{}^1FNIII)_4$ protein (284 nm). (b) Histogram of contour length increases, ΔL_c, observed in the $(I27-{}^1FNIII)_4$ protein. There are three clearly separated distributions centered at 9 nm ($9.3(\pm 1.6)$ nm, $n = 12$), at 20 nm ($20.1(\pm 1.7)$ nm, $n = 57$) and at 28 nm ($27.8(\pm 1.1)$ nm, $n = 145$). (c) Unfolding force histogram for force-peaks contributing to increases in contour length, ΔL_c, of 9 nm, 20 nm and 28 nm. The average unfolding forces are 90 pN ($91(\pm 23)$ pN, $n = 12$), 120 pN ($125(\pm 41)$ pN, $n = 57$) and 200 pN ($206(\pm 21)$ pN, $n = 145$), respectively.

boundary was from Thr625 to Thr722 (97 residues). This construct included five residues in its N terminus that are considered to be the linker region between ^{9}FNI and ^{1}FNIII[38] but excluded the 18 residue linker between the C terminus of the ^{1}FNIII domain and the N terminus of the ^{2}FNIII domain. We designated this sequence, lacking the C terminus linker, as the "classic" ^{1}FNIII domain. We also made a construct that included the 18 residue linker to test whether its presence altered the mechanical stability of the module. We made a polyprotein that, in addition to the classic ^{1}FNIII module, contained both the 18 residue linker and its natural neighbor, the ^{2}FNIII domain. In this polyprotein (^{1}FNIII–^{2}FNIII), the ^{1}FNIII module has its "native" configuration. We compare the mechanical stability of the ^{1}FNIII module defined by these various boundaries. In addition to testing the effect of the C terminus extensions on the mechanical stability of ^{1}FNIII, we tested whether the N terminus linkage between ^{9}FNI and ^{1}FNIII (see the inset in Figure 1) played a role in the mechanical stability of the ^{1}FNIII module.

The classic ^{1}FNIII domain displays low mechanical stability and partially folded intermediates

To determine the mechanical unfolding behavior of the classic ^{1}FNIII module, we used a protein chimera strategy where a domain with a known mechanical property (titin immunoglobulin domain I27) is combined with a domain of unknown structure.[30,39] The I27 modules introduce an internal fingerprint that can be identified readily by AFM, facilitating the identification of the unknown domains. Figure 2 shows force–extension curves measured in a protein composed of four repeats of a I27–^{1}FNIII dimer, $(I27-{}^1FNIII)_4$. A prominent feature of these recordings is a long spacer preceding several force-peaks (Figure 2(a), a–e). The continuous lines are fits of the worm-like-chain (WLC) equation[40] to the data. Figure 2(a), a shows a common pattern observed for the $(I27-{}^1FNIII)_4$ protein: a force–extension curve with a long spacer followed by four force-peaks. These four peaks have the fingerprint of

the unfolding pattern of the titin immunoglobulin domains.[24,30,39,41] Given the construction of the (I27–¹FNIII)₄ polyprotein (Figure 2(a), left inset), if four I27 unfolding peaks are observed at least three ¹FNIII domains must have been stretched. The contour length to the first force-peak, L_o, is ~155 nm (154($\pm$18) nm, $n = 14$), a value that is consistent with four unfolded ¹FNIII domains (97 residues × 4 domains × 0.38 nm/residue = 147 nm). This result suggests that, in these types of recordings, all four ¹FNIII domains are already unfolded before stretching. Alternatively, ¹FNIII domains may have a very low mechanical stability with unfolding forces that are below the limit of our resolution (~20 pN). These results are similar to those from the AFM studies of barnase.[30] Those authors used an I27–barnase polyprotein and found that barnase does not show a discernible fingerprint of unfolding peaks, although both modules were found to be folded independently in this construct.[30]

We observed sawtooth patterns with more than four force-peaks (Figure 2(a), b–e). Figure 2(a), b and c show recordings with one or two force-peaks before the unfolding of the four I27 domains. These peaks have a lower force (~100 pN) and with a shorter unfolded length (~20 nm), than the I27 force-peaks. Figure 2(a), d shows a more complex sawtooth pattern with three peaks before the four I27 unfolding events. The spacing are 20, 8 and 20 nm. In some rare cases (two out of 250 recordings), we observed sawtooth patterns with five force-peaks all spaced by 28 nm (Figure 2(a), e). Since all these recordings contain the fingerprint marker for the unfolding of the I27 domains, these additional force-peaks must represent the unfolding of ¹FNIII domains. These recordings show a spacer before the first force-peak, suggesting that several ¹FNIII domains in the polyprotein were already unfolded before stretching it. These results suggest that the classic ¹FNIII domain in the I27–¹FNIII polyprotein can be either unfolded (i.e. forming a structure that is not mechanically resistant similar to a random coil), or forming stable folds that harbor different numbers of amino acid residues.

We calculated the number of amino acid residues exposed upon unfolding by measuring the increase in contour length, ΔL_c, contributed by each unfolding event. Figure 2(b) shows that there are three clearly separated distributions for ΔL_c in the I27–¹FNIII polyprotein: one centered at 9 nm (9.3($\pm$1.6) nm, $n = 12$), another at 20 nm (20.1($\pm$1.7) nm, $n = 57$) and one at 28 nm (27.8($\pm$1.1) nm, $n = 145$). This last distribution corresponds to the unfolding of the I27 domains (including the two recordings similar to Figure 2(a), e). An increase in contour length, ΔL_c, of 28 nm corresponds to the unraveling of a structure containing about 75 amino acid residues, ΔL_c of 20 nm corresponds to the unraveling of 53 amino acid residues and ΔL_c of 9 nm to the unraveling of about 23 amino acid residues. Thus, the data

suggest that the ¹FNIII domain exhibits several partially folded intermediates containing either 53 or 23 amino acid residues in the folded structure.

The different partially folded structures of the classic ¹FNIII domain have distinct mechanical stability. Figure 2(c) shows a histogram for the unfolding forces of events giving an increase in contour length of 9 nm, 20 nm and 28 nm. The force-peaks producing the shortest ΔL_c have an average unfolding force of 90 pN (91($\pm$23) pN, $n = 12$), whereas the force-peaks giving an ΔL_c of 20 nm show an average unfolding force of 125 pN (125($\pm$41) pN, $n = 57$). The distribution on the right corresponds to the unfolding forces of the I27 domains (206($\pm$21) pN, $n = 145$). Hence, the partially folded structure of ¹FNIII containing the smallest number of amino acid residues is mechanically the weakest.

Our results indicate that the classic domain ¹FNIII can have several mechanically stable conformations. In the absence of its natural FNIII neighbor domain, it can be either already unfolded, or forming mechanically resistant structures that harbor different number of amino acids (Figures 2 and 3). It interesting to note that similar unfolding intermediates have been predicted by molecular dynamics simulations done on FNIII domains.[15,16] Biased molecular dynamics simulations done on ⁹FNIII and ¹⁰FNIII domains of fibronectin[15] and on the ³FNIII domain of tenascin[16] revealed that these domains unfold in steps, where each step corresponds to the peeling off of one or more β-strands from the fold. According to the molecular dynamics simulations, the first intermediate will be reached after stretching the domain by 9.6 nm and a second intermediate is reached at ~15 nm, before full unfolding at 28.1 nm.[15] These predictions are similar to our experimental data.

The native ¹FNIII is mechanically very stable

In order to examine the mechanical properties of the ¹FNIII domain with its natural neighbor and linker sequence, we constructed a protein containing several repeats of the ¹FNIII–²FNIII dimer, (¹FNIII–²FNIII)₆. Figure 3 shows the result of stretching a (¹FNIII–²FNIII)₆ polyprotein. In contrast to the I27–¹FNIII polyprotein, there is no spacer before the force-peaks. Figure 3(a) shows examples of the most common sawtooth patterns observed; the force-peaks are evenly spaced by a ΔL_c of 28 nm and with unfolding forces of 220 pN (220($\pm$44) pN, $n = 205$; Figure 3(e)). This indicates that all the domains in this protein have a high mechanical stability. Although the protein contains 12 domains, the maximum number of force-peaks we have observed is eight (Figure 3(a)). This is because the AFM tip picks up the proteins at a random location, resulting in sawtooth patterns with a varying number of peaks.[33] However, since the polyprotein is constructed in an alternating ¹FNIII–²FNIII pattern, if eight peaks are observed, then there must be four events that correspond to
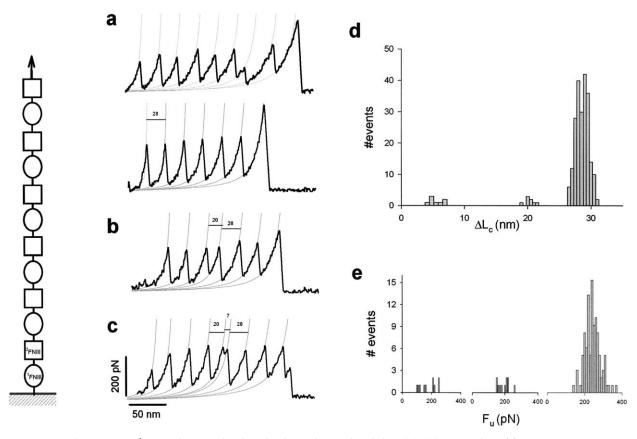
Figure 3. The "native" ^{1}FNIII domain displays high mechanical stability. (a)–(c) Examples of force–extension curves for an (^{1}FNIII–^{2}FNIII)$_6$ polyprotein. (a) Examples of sawtooth patterns with eight or with six equally spaced force-peaks with ΔL_c of 28 nm. (b) and (c) Examples of sawtooth patterns displaying different values for ΔL_c. (d) Histogram for the increases in contour length observed in the (^{1}FNIII–^{2}FNIII)$_6$ polyprotein: ΔL_c shows three discrete values, at 9 nm (9.2($\pm$0.8) nm, $n = 8$), at 20 (20.2($\pm$0.7) nm, $n = 11$) and at 28 nm (28.3($\pm$2.5) nm, $n = 207$). (e) Unfolding force histogram for force-peaks contributing to increases in contour length, ΔL_c, of 9 nm, 20 nm and 28 nm. The unfolding forces for the three types of events are 178($\pm$51) pN ($n = 8$), 193($\pm$35) pN ($n = 11$) and 220 ($\pm$44) pN ($n = 205$).

the unfolding of one type of module and four of the other type. Hence, in this protein the ^{1}FNIII and ^{2}FNIII domains have an identical mechanical stability.

We observed evidence of partially folded intermediates in the (^{1}FNIII–^{2}FNIII)$_6$ polyprotein (Figure 3(b) and (c)), but these events occur at a low frequency (19 out 167 sawtooth patterns). Figure 3(b) shows an example of a sawtooth pattern with five unfolding events that increased ΔL_c by 28 nm, and one event that increased ΔL_c by 20 nm. In the example illustrated by Figure 3(c) there are ten force-peaks, six that increase ΔL_c by 28 nm, two by 20 nm and two that increase ΔL_c by 9 nm. As shown by the histogram in Figure 3(d), the increase in contour length, ΔL_c, shows three discrete values, at 9 nm (9.2($\pm$0.8) nm, $n = 8$), at 20 (20.2($\pm$0.7) nm, $n = 11$) and at 28 nm (28.3($\pm$2.5) nm, $n = 207$). These values of ΔL_c are identical with those observed in the (I27–^{1}FNIII)$_4$ protein, suggesting that these events are likely to correspond to the unfolding of partially folded ^{1}FNIII domains. However, in contrast to the classical ^{1}FNIII domain, the partially folded intermediates observed in the native ^{1}FNIII domain all

have higher unfolding forces ($\sim$ 200 pN; Figure 3(e)) and occur at much lower frequency and with no indication of unfolded domains.

Effect of the linkers on the mechanical stability of ^{1}FNIII

It is not clear what type of interactions could be stabilizing the ^{1}FNIII domain in the (^{1}FNIII–^{2}FNIII)$_6$ polyprotein. It could be a direct interaction between the folded domains as shown for ^{9}FNIII and ^{10}FNIII domains[12] and titin Ig domains I27 and I28[42] or an effect of the linker region between domains as previously shown for a FNIII domain.[37] For example, Hamill *et al.*[37] showed that extending the C terminus of an ^{3}FNIII domain by only two residues decreased the unfolding rate by 40-fold.

The linker region between the ^{1}FNIII and ^{2}FNIII dimer is unusual in that it is very long, containing 18 residues. The results obtained with the ^{1}FNIII–^{2}FNIII dimer polyprotein suggested that the native linker maybe important for the proper folding of ^{1}FNIII, which results in an increase in the mechanical stability of ^{1}FNIII in this construct
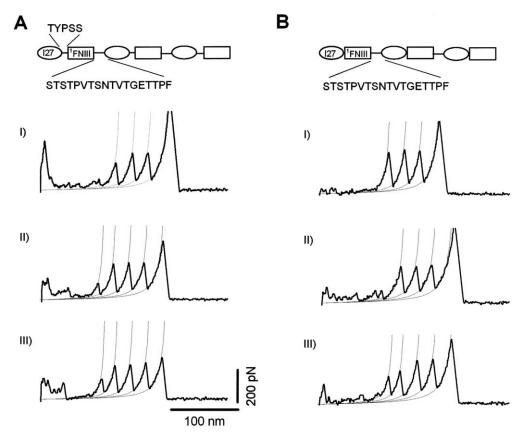
Figure 4. Effect of the linker sequences on the mechanical stability of the ¹FNIII domain. (a) Examples of force–extension curves obtained from an (I27–¹FNIII)₃ polyprotein that includes the native ¹FNIII C terminus linker sequence (STSTPVTSNTVTGETTPF). (I) Example of a sawtooth pattern showing a long spacer followed by the unfolding the three I27 domains (consecutive force-peaks at ~ 200 pN and equally spaced by ~ 28 nm). (II–III) Examples of sawtooth patterns with four clear force-peaks, where the first unfolding event occurs at a low force and shows a ΔL_c of ~ 20 nm and the next unfolding events all have a ΔL_c of 28 nm. (b) Examples of force–extension curves obtained from a (I27–¹FNIII)₃ that includes the native C terminus sequence but lacks the five amino acid residues in the N terminus that serve as the linker with ⁹FNI. Similar to the data shown in (a), the force–extension curves show the three I27 unfolding force-peaks, preceded by a spacer ((I), (II)) or additional force-peaks that contribute with a ΔL_c of 20 nm (III).

(Figure 3). Hence, it is possible that the linker in the (I27–¹FNIII)₄ polyprotein is too short to allow the ¹FNIII to fold properly. To test whether the C terminus linker increases the mechanical stability of the ¹FNIII domain, we constructed an I27–¹FNIII polyprotein containing the complete C terminus linker region. Figure 4(a) shows several examples of force–extension curves obtained from a (I27–¹FNIII)₃ polyprotein that includes the native C terminus linker sequence (STSTPVTSNTVTGE-TTPF). The boundaries for ¹FNIII in this construct are identical with those in the ¹FNIII–²FNIII dimer polyprotein (Figure 3). However, the inclusion of the native C terminus linker in the ¹FNIII does not result in a more stable domain. As Figure 4(a) shows, stretching a (I27–¹FNIII-native linker)₃ polyprotein results in force–extension curves containing the three I27 domains (the three force-peaks before the final detachment force-peak), which are preceded by either a long spacer (Figure 4(a), a) or few additional unfolding events that contribute to an increase in ΔL_c of ~ 20 nm (Figure 4(a), b and c), indicating that the ¹FNIII domains

are mechanically very weak or partially folded, similar to what we observed in the absence of the linker region. Hence, adding the native C terminus linker does not increase the mechanical stability of ¹FNIII.

The classic ¹FNIII sequence contains five additional residues (TYPSS) that form the N terminus linker sequence with ⁹FNI.[38] To test the role of this linker in the mechanical stability of ¹FNIII, we constructed an I27–¹FNIII polyprotein lacking these five residues. As Figure 4(b) shows, the AFM recordings are very similar to those shown in Figures 2 and 4(a), showing that removal of these five residues does not affect the mechanical stability of the classic ¹FNIII.

Hence, our data suggest that the observed stabilization of the ¹FNIII in the ¹FNIII–²FNIII dimer polyprotein does not result from a contribution of the linker sequences. The stabilization of ¹FNIII may result from unknown domain–domain interactions or it is possible that the ²FNIII domain acts like a chaperone and is needed as a neighbor for the correct folding of ¹FNIII.
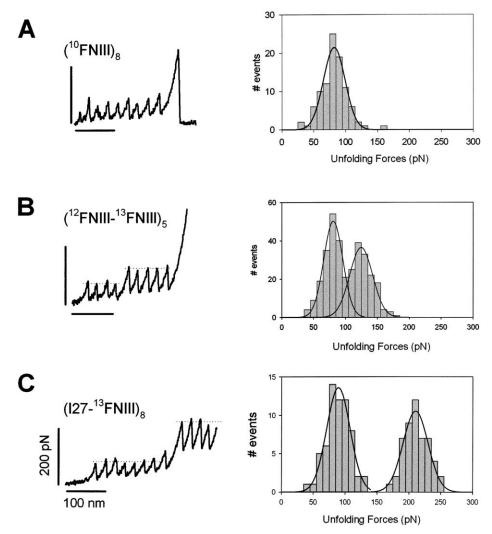
Figure 5. The mechanical stability of domains ^{10}FNIII, ^{12}FNIII and ^{13}FNIII. (a) Stretching (^{10}FNIII)$_8$ polyproteins resulted in force–extension curves with sawtooth patterns revealing unfolding forces of $\sim$75 pN (74($\pm$20) pN, $n = 97$; unfolding force histogram on the right panel). (b) Stretching the (^{12}FNIII–^{13}FNIII)$_5$ polyprotein resulted in sawtooth patterns with two levels of unfolding forces, the first was observed at 82 pN (81.7($\pm$14) pN, $n = 201$) and the second at 125 pN (124($\pm$18) pN, $n = 123$). (c) Sawtooth patterns obtained from the (I27–^{13}FNIII)$_8$ polyprotein shows two levels of unfolding forces (see the histogram on the right panel) one centered at $\sim$90 pN (89($\pm$18) pN, $n = 64$), which corresponds to the unfolding of ^{13}FNIII, and a second at $\sim$200 pN (209($\pm$19) pN, $n = 51$), which is the characteristic value of I27 unfolding.

The ^{10}FNIII domain has a low mechanical stability

In order to determine the mechanical properties of the ^{10}FNIII domain, we constructed a polyprotein with identical repeats of the ^{10}FNIII domain. As Figure 5(a) shows, stretching the (^{10}FNIII)$_8$ polyprotein results in a sawtooth pattern with force-peaks that varied about an average value of 75 pN (74($\pm$20) pN, $n = 97$; Figure 5(a), right panel). This places the ^{10}FNIII domain in the lower range of the domain unfolding hierarchy in fibronectin. Steered molecular dynamics simulations had predicted that ^{10}FNIII was mechanically weaker than ^{7}FNIII, ^{8}FNIII and ^{9}FNIII.[18] We could not verify these predictions directly because we did not succeed in constructing polyproteins based on these modules. However, given that our data shows that

^{10}FNIII would be the first module to unfold under a stretching force, it is likely that FNIII domains 7, 8, and 9 will indeed be more stable than domain 10, as predicted by the SMD simulations.[18]

The mechanical stability of domains ^{12}FNIII and ^{13}FNIII

Figure 5(b) shows a force–extension curve of a (^{12}FNIII–^{13}FNIII)$_5$ polyprotein. There are two levels of unfolding forces, one at $\sim$80 pN (81.7($\pm$14) pN; $n = 201$) and a second at $\sim$120 pN (124($\pm$18) pN; $n = 123$; Figure 5(b) B, right panel). Hence, FNIII domains 12 and 13 have significantly different unfolding forces. However, we do not know which domain unfolds first, ^{12}FNIII or ^{13}FNIII.

To determine the origin of the observed unfolding forces in the (^{12}FNIII–^{13}FNIII)$_5$ polyprotein, we
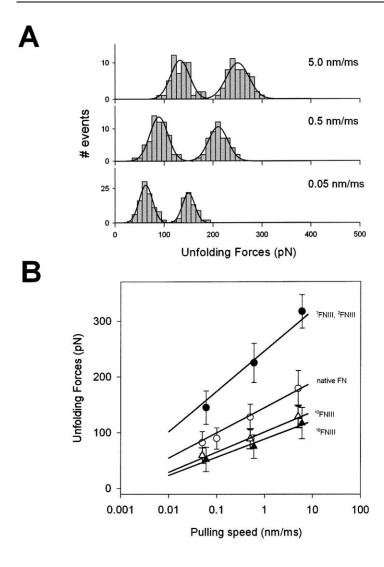
A

B

Figure 6. Kinetics of unfolding of single FNIII domains. (a) Distribution of unfolding forces of the (I27–^{13}FNIII)$_8$ polyprotein obtained at three different pulling speeds. The two clearly separated peaks in the distribution correspond to the force required to unfold ^{13}FNIII (low force) and I27 (high force). The distributions are repeated at three different pulling rates. (b) Plot of the average unfolding force *versus* the pulling rate for FNIII domains 1, 2 (filled circles), native fibronectin (open circles), FNIII domain 13 (open triangles), FNIII domain 10 (filled triangles). The error bars correspond to the standard error of the mean. The continuous lines correspond to the result of Monte Carlo simulations of two-state unfolding at the corresponding pulling rates. The parameters used for the Monte Carlo simulation are shown in Table 1.

constructed a protein chimera of ^{13}FNIII with the titin I27 immunoglobulin domain. As Figure 5(c) shows, the force–extension curves show two very clear levels of unfolding forces, one at 90 pN (89($\pm$18) pN, $n = 64$) and a second at 200 pN (209($\pm$19) pN, $n = 51$; Figure 5(c), right panel). Since, the last four peaks in the recording shown in Figure 5(c) have the fingerprint of the unfolding pattern of the titin I27 domains (regular spacing of $\sim$28.1 nm and an unfolding force of $\sim$200 pN), the low force-peaks must correspond to the unfolding of ^{13}FNIII domains. This experiment shows that the ^{13}FNIII domain has a relatively low unfolding force of $\sim$90 pN. Since this value is similar to the low force level observed in the (^{12}FNIII–^{13}FNIII)$_5$ protein (Figure 5(b)), we can now conclude that the ^{12}FNIII domain is mechanically more stable than the ^{13}FNIII domain ($\sim$120 pN and $\sim$90 pN, respectively).

The rate dependency of mechanical unfolding varies greatly amongst FNIII modules

Our results show that FNIII domains of fibronectin have very different unfolding forces, which vary from 75 pN (for ^{10}FNIII domains) to 220 pN (for ^{1}FNIII and ^{2}FNIII domains). These values were obtained at a fixed pulling speed (0.6 μm/ second). However, during cell–cell interactions these domains may experience a wide range of stretching speeds. Since the mechanical stability may not be the same at different pulling speeds, as shown for titin domains,[19,24] we studied the rate-dependency of the stability of FNIII domains.

Figure 6(a) shows an example of the distribution of unfolding forces of the (^{13}FNIII–I27)$_8$ polyprotein obtained at three different pulling speeds. The two clearly separated peaks, corresponding to the unfolding forces of ^{13}FNIII (low force) and I27 domains (high force), are shown to depend on the pulling speed. A tenfold decrease in pulling speed decreases the unfolding forces of both types of domains by about the same amount, $\sim$45 pN. Figure 6(b) compares the relationship between the unfolding force and the pulling speed (0.05– 6 nm/ms) for different FNIII domains. The average unfolding force for FNIII domains 10 (filled triangles) and domains 13 (open triangles) are weakly dependent on the pulling speed, whereas domains 1 and 2 show a stronger dependence (filled circles).

Table 1. Summary of the kinetic and mechanical properties of single FNIII domains

	F_u (pN) (at 0.6 nm/ms)	k_U^0 (s^{-1})	$\Delta G^{F=0}$ (kcal/mol)	Δx_U (nm)	k_F^0 (s^{-1})
^{1}FNIII	220	4.0×10^{-3}	20.5	0.17	–
^{2}FNIII	220	4.0×10^{-3}	20.5	0.17	–
^{10}FNIII	75	2.0×10^{-2}	22.2	0.38	0.9
^{12}FNIII	125	–	–	–	0.8
^{13}FNIII	89	2.2×10^{-2}	19.5	0.34	0.8

The unfolding rates at zero force, and the unfolding distance, Δx_U, were determined from Figure 6(b) and the refolding rates constant at zero force, k_{F0}, from Figure 7(b). $\Delta G^{F=0}$ is the free energy calculated from the unfolding rates at zero force using a pre-factor of 6×10^{12} s^{-1}.

The unfolding of native fibronectin shows a dependence on the pulling speed that is between those for ^{1}FNIII and ^{10}FNIII. This relationship was used to determine the unfolding rate constants for these domains using a Monte Carlo simulation technique to simultaneously predict the distribution of their unfolding forces and their speed dependency.[24] The estimated values for the unfolding rates at zero force were 4×10^{-3} s^{-1}, 4×10^{-3} s^{-1}, 2×10^{-2} s^{-1} and 2.2×10^{-2} s^{-1}, and unfolding distances of 0.17, 0.17, 0.38, 0.34 nm for FNIII domains 1, 2, 10, and 13, respectively (Table 1). These results show that the mechanical hierarchy of FNIII domains is conserved over a wide range of pulling speeds.

As shown in Table 1, the calculated activation energies are very similar between the different domains but the unfolding distances vary significantly (from 0.17 nm for ^{1}FNIII to 0.38 nm for ^{10}FNIII). The unfolding distance Δx corresponds to the distance over which mechanical work must be done in order to trigger the unfolding event[19,24,43] and, in an energy diagram, is related to the position of the transition state.[24,44] Hence, the differences in the mechanical stability of the different FNIII domains studied here seem to arise mainly from changes in the position of the transition state of the mechanical energy landscape.[24]

Fibronectin FNIII domains refold at very similar rates

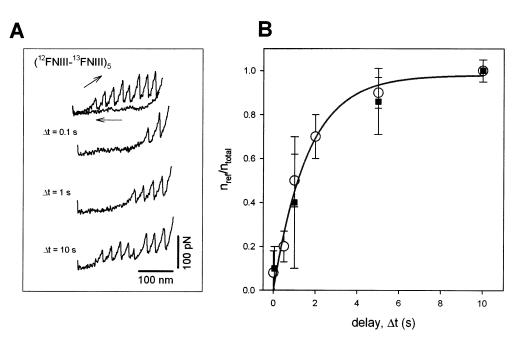During mechanical interactions with cells, it is likely that fibronectin domains are unfolding and

Figure 7. FNIII domains readily refold after mechanical unfolding. (a) Unfolding and refolding cycles obtained from a single (^{12}FNIII–^{13}FNIII)$_5$ polyprotein probed with a double-pulse protocol. The protein is first stretched to count the number of domains that unfold, n_{total}, (top trace marked by forward arrow), and then it is relaxed to its initial length (backward arrow). Subsequent extensions after a delay, Δt, measure the number of refolded domains, n_{ref}. Three examples are shown where Δt was increased from 100 ms (second trace), then to one second (third trace) and then to ten seconds (bottom trace). (b) Plot of the refolded fraction, n_{ref}/n_{total} *versus* Δt, for ^{10}FNIII (filled squares) and ^{12}FNIII, ^{13}FNIII domains (open circles). The continuous line corresponds to a fit of the ^{12}FNIII, ^{13}FNIII refolding data to an exponential function, where $k_f^0 = 0.6$ s^{-1}.

refolding continuously. In order to test if FNIII domains refold after mechanical unfolding, we used a two-pulse stretching protocol to repeatedly stretch and relax a single protein.[23,24] Figure 7(a) shows a typical refolding experiment where a single (^{12}FNIII–^{13}FNIII)$_5$ polyprotein remained attached to an AFM tip allowing for repeated extension and relaxation cycles (up to 50 cycles in this experiment). Since the polyprotein is picked at a random length and the total extension of the protein is limited to prevent detachment, the number of extended domains is typically less than the maximum. Four consecutive traces are shown. A first extension of the protein revealed eight regularly spaced force-peaks corresponding to the unfolding of ^{12}FNIII and ^{13}FNIII domains (Figure 7(a); top trace). Then, by moving back the tip of the AFM cantilever, the protein was relaxed to its original length. After a variable period ($\Delta t = 0.1$ second, one second and ten seconds, Figure 7(a)), the protein was stretched again and several force-peaks were observed. This indicates that some of the unfolded domains had refolded spontaneously upon relaxation. Notice the two levels of unfolding forces in the sawtooth patterns; the lower level corresponds to the unfolding of ^{13}FNIII domains. These domains were seen to refold with similar rates. Figure 7(b) shows a plot of the refolded fraction, n_{ref}/n_{total} *versus* Δt for ^{10}FNIII (filled squares), ^{12}FNIII, ^{13}FNIII domains (open circles). We observed that the number of FNIII domains refolded, after a complete unfolding, recovered with an exponential time-course, as observed for titin Ig domains.[19,24] The continuous line is a fit of the data to an exponential function, where $k_{F0} = 0.6\,s^{-1}$. Thus, different FNIII domains in fibronectin refold with similar rate constants, although they have widely varying mechanical stability.

Discussion

Understanding the role of mechanical force in regulating extracellular matrix assembly requires an understanding of the conformational changes that proteins undergo in response to a stretching force. Using single-molecule AFM, we found that fibronectin is highly extensible and that this extensibility is due to the unfolding of its FNIII domains. Stretching native fibronectin results in a sawtooth pattern with equally spaced force-peaks that have a wide range of unfolding forces (Figure 1). By combining single-molecule force spectroscopy and protein engineering techniques, we demonstrate here that the sawtooth pattern in native fibronectin corresponds to the sequential unfolding of individual FNIII domains. We found that FNIII domains refold readily after mechanical unfolding. Hence, fibronectin displays a dynamic extensibility whereby the resting length might be regulated through domain unfolding and refolding. The complete unfolding of the FNIII region of a single

fibronectin dimer (which contains 28 FNIII domains) would extend the molecule by about sixfold from a folded length of about 160 nm,[45] to an unfolded, stretched-out length of 950 nm (28 domains × 28.1 nm contour length increase). This remarkable extensibility of fibronectin may render the extracellular matrix unbreakable when pulled beyond its physiological range. This function might be important for tissue preservation under deforming loads.

One of the salient features of the AFM experiments with native fibronectin is the hierarchical unfolding of its domains (Figure 1). In order to understand the molecular basis of the unfolding hierarchy, we examined the mechanical properties of individual FNIII modules. Figure 8 summarizes the results obtained for the mechanical stability of FNIII domains. This plot relates the height of the force-peak with its position in the sawtooth pattern in native fibronectin (inset). This Figure shows that domains containing cell-binding sites (^{10}FNIII and ^{13}FNIII) are mechanically the weakest domains showing low unfolding forces (~ 80 pN), and that FNIII domains 1 and 2 are mechanically the most stable (with unfolding forces of ~ 220 pN). These results contradict chemical and thermal measurements of stability, which found that ^{10}FNIII is very stable with a thermal stability of 102 °C,[11] with an unfolding rate at zero denaturant of $k_U^{H_2O}$ of $2.3 \times 10^{-4}\,s^{-1}$.[14] We found that ^{10}FNIII is mechanically weak and has an unfolding rate at zero force k_U^0 of $2 \times 10^{-2}\,s^{-1}$ (Table 1). Our studies demonstrate the importance of directly measuring mechanical stability, which does not correlate well with either thermal or chemical stability, in proteins that are known to function under a stretching force.

Studies using analytical affinity chromatography techniques have suggested that the ^{1}FNIII domain exists in a partially unfolded form that is ready to promote the self-assembly of a fibronectin matrix at a low stretching force.[4,8,9] In agreement with this observation, we found that the ^{1}FNIII domain is mechanically very unstable and shows several partially folded conformations (Figures 2 and 4). However, we found that the neighbor FNIII domain dramatically affects the stability of ^{1}FNIII (Figure 3), suggesting that ^{1}FNIII is very stable in the native fibronectin protein and that the putative cryptic buried in the fold of ^{1}FNIII might not be exposed under a stretching force. This is supported by recent observations showing that ^{1}FNIII is not essential for fibrillogenesis, and that there seems to be a second binding site in ^{2}FNIII.[10] Furthermore, these authors propose that $^{1-2}$FNIII may act in concert to promote self-assembly, and that interactions between domains 1 and 2 regulate the accessibility of the cryptic binding site.[10] This latter model is very attractive, because the force required to expose this cryptic binding site would be very low, as compared to the force required for the full unfolding of the modules.
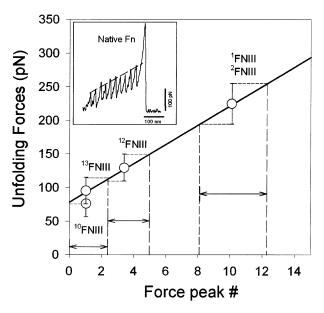
Figure 8. The mechanical hierarchies of fibronectin FNIII domains. The plot shows the rising forces required to trigger the unfolding of consecutive FNIII domains in native fibronectin. The inset shows a recording from a native fibronectin protein. From the measured force required to trigger their unfolding, we can order the FNIII domains by their mechanical stability. The symbols show the relative position of the FNIII domains in the mechanical hierarchy in fibronectin.

Can cells develop large enough forces to unfold FNIII domains in fibronectin? Several studies have demonstrated that cells can generate a con- siderable amount of mechanical tension on the substratum.[46−48] Using elastic micropatterned substrates, it was shown that a single cell can generate traction forces of up ∼70 nN and forces of ∼5 nN/μm^2 at their single focal adhesion points.[48] If a crystalline packing is assumed at the focal adhesion (∼1000 integrins/μm^2), single fibro- nectin molecules would be subjected to forces of about 1 pN, although this estimation constitutes a lower limit and the forces per molecule might be much higher.[48] Since domain unfolding and refolding depends exponentially on the applied force, even a small force of a few picoNewtons will increase the unfolding probability by several orders of magnitude.[24,34,35] For example, a force of only 15 pN will increase the unfolding rate of domain ^{10}FNIII to about one unfolding event every six seconds. Also, the unfolding forces of FNIII domains would depend on the speed at which the molecules are being stretched, where a tenfold decrease in pulling speed will decrease the unfolding forces by as much as 100 pN (Figure 6). Since cells typically crawl at speeds of 0.01– 0.1 μm/second,[46−48] FNIII domains are predicted to unfold at low forces (e.g. domain ^{10}FNIII would unfold at force of a few picoNewtons when pulled at 0.01 μm/second; Figure 6). In support of this possibility, experiments with a fibronectin-green

fluorescent protein chimera have demonstrated that fibronectin is highly extended by about four times their resting length. The authors suggested that the extensibility of fibronectin could arise from either domain unfolding or the elongation of compacted fibronectin fibrils.[49] Recent studies using fluorescence energy transfer on fibronectin further support the hypothesis that FNIII domains do unfold under physiological conditions.[50] Finally, studies of cell adhesion at the single-molecule level have shown that receptor–ligand bonds are challenged by forces in the range between 100 and 200 pN during cell adhesions interactions.[51,52]

Hence, it is possible that fibronectin, due to its intimate interaction with cells, must itself be under mechanical tension, and that FNIII domains are likely to unfold during the mechanical inter- actions between cells. Our data show that FNIII domains of fibronectin will unfold in a hierarchical manner (Figure 8): FNIII domains 10 and 13 would be the first to unfold, followed by FNIII domain 12, and FNIII domains 1 and 2, will be the last FNIII domains to unfold. The hierarchical unfolding of FNIII domains may have the result of considerably decreasing the affinity of fibronectin for cell recep- tors, leading to the rapid unbinding of fibronectin from cells and other molecules. At the same time, the application of a mechanical force may trigger the exposure of new binding sites that were buried between domains or in the fold also promote the binding of other fibronectin molecules.[4,8,9,10,49,53] Hence, domain unfolding in fibronectin modulates its resting length and elasticity, and it may modu- late its cell-binding properties significantly.[17,53,54] These force-triggered events might be important for the activation of fibrillogenesis and matrix assembly.

Materials and Methods

Construction of (I27−^{1}FNIII)$_4$, (^{1}FNIII−^{2}FNIII)$_6$, (I27−^{10}FNIII)$_4$, (^{10}FNIII)$_8$, (I27−^{13}FNIII)$_8$, (^{12}FNIII−^{13}FNIII)$_5$ and (I27)$_8$ polyproteins

We used two strategies to construct polyproteins based on FNIII domains. In the first method, we con- structed protein chimeras where we linked an FNIII domain with a domain of known mechanical stability, i.e. the 27th immunoglobulin module of human cardiac titin.[24,25,33] We assembled (I27−^{1}FNIII)$_x$, (I27−^{10}FNIII)$_4$ and (I27−^{13}FNIII)$_8$ chimeras using a multiple-step cloning technique[24,25] that makes use of four restriction sequences (*Bam* HI, *Bgl* II, *Bst* Y and *Kpn* I) to build even multiples of the I27–^{x}FNIII domains. We constructed polyproteins made of identical repeats of a single FNIII domain or of two neighboring domains (^{1}FNIII–^{2}FNIII)$_6$, (^{10}FNIII)$_8$, (^{12}FNIII–^{13}FNIII)$_5$ and titin I27 domain, (I27)$_8$, by using directional DNA concatemerization by self- ligation of the sticky ends of the non-palindromic *Ava* I restriction site.[24,25] We attempted to make polyproteins for other FNIII domains like ^{7}FNIII, ^{8}FNIII, ^{9}FNIII, or from dimers like ^{7}FNIII–^{8}FNIII and ^{9}FNIII–^{10}FNIII, but we encountered difficulties with the expression of these constructs. The polyproteins were cloned in an

Escherichia coli recombination-defective strain, Sure-2 (Stratagene), and expressed in the BLR (DE3) strain (Novagene). The proteins were lysated using a French press or by the use of Triton X-100 and then purified by Ni^{2+} or Co^{2+} affinity chromatography. All these proteins had two Cys in their C terminus to facilitate the attachment of the molecules to the gold-coated coverslips. The proteins were kept in PBS containing 5 mM DTT and 0.2 mM EDTA at 4 °C.

We selected the boundaries for FNIII domains 10, 12, 13 on the basis of the crystal structures for these domains.[7,36] The boundaries are as follows: [10]FNIII has 94 residues (from Val1559 to Thr1653), [12]FNIII has 92 residues (from Ala1833 to Glu1925) and [13]FNIII has 89 residues (from Asp1926 to Thr2015). The boundary selection of FNIII domains 1 and 2 is more uncertain because of the lack of structural information for these domains. We used the following boundaries for these domains: [1]FNIII from Thr625 to Thr722 (97 residues) and [2]FNIII from Ser739 to Thr830 (91 residues). This leaves an 18 residue linker between the C terminus of the [1]FNIII domain and the N terminus of the [2]FNIII domain. We constructed several [1]FNIII polyproteins based on different selection for the boundaries of [1]FNIII. The [1]FNIII sequence lacking the C terminus linker we designated as the classic [1]FNIII domain. This sequence includes five residues in its N terminus that are considered[38] to be the linker region between [9]FNI and [1]FNIII.[42] We constructed additional I27–[1]FNIII polyproteins, which included the complete native C terminus linker sequence, STSTPVTS-NTVTGETTPF ([Figure 4(a)]) and another lacking the five N terminus residues in [1]FNIII ([Figure 4(b)]). We constructed a polyprotein for the [1]FNIII–[2]FNIII dimer (starting in Thr625 and ending in Thr830). The [1]FNIII domain in this construct we termed as the native [1]FNIII domain.

Atomic force microscopy

Our single-molecule force spectroscopy methods have been described.[23,24,29] The cantilevers used in this study were Si_3N_4 cantilevers from Digital Instruments (with a typical spring constant of $\sim 100\ mN\ m^{-1}$) and from ThermoMicroscopes (with a typical spring constant of $\sim 45\ mN\ m^{-1}$), respectively. Calibration of the cantilevers was done in solution and using the equipartition theorem.[55,56] Unless noted in the text, all force–extension curves were obtained at a pulling speed of 0.6 μm/second.

References

1. Halliday, N. L. & Tomasek, J. J. (1995). Mechanical properties of the extracellular matrix influence fibronectin fibril assembly *in vitro*. *Expt. Cell Res.* **217**, 109–117.
2. Shaub, A. (1999). Unravelling the extracellular matrix. *Nature Cell Biol.* **1**, E173–E175.
3. Schwarzbauer, J. E. & Sechler, J. L. (1999). Fibronectin fibrillogenesis: a paradigm for extracellular matrix assembly. *Curr. Opin. Cell Biol.* **11**, 622–627.
4. Zhong, C., Chrzanowska-Wodnicka, M., Brown, J., Shaub, A., Belkin, A. M. & Burridge, K. (1998). Rho-mediated contractility exposes a cryptic site in fibronectin and induces fibronectin matrix assembly. *J. Cell Biol.* **141**, 539–551.
5. Hynes, R. O. (1999). The dynamic dialogue between cells and matrices: implications of fibronectin's elasticity. *Proc. Natl Acad. Sci. USA*, **96**, 2588–2590.
6. Johanssen, S., Svineng, G., Wennerberg, K., Armulik, A. & Lohikangas, L. (1997). Fibronectin–integrin interactions. *Frontiers Biosci.* **2**, 126–146.
7. Sharma, A., Askari, J. A., Humphries, M. J., Jones, E. Y. & Stuart, D. I. (1999). Crystal structure of a heparin- and integrin-binding segment of human fibronectin. *Eur. Mol. Biol. Org. J.* **18**, 1468–1479.
8. Ingham, K. C., Brew, S. A., Huff, S. & Litvinovich, S. V. (1997). Cryptic self-association sites in type III modules of fibronectin. *J. Biol. Chem.* **272**, 1718–1724.
9. Hocking, D. C., Sottile, J. & McKeown-Longo, P. J. (1994). Fibronectin's III-1 module contains a conformation-dependent binding site for the amino-terminal region of fibronectin. *J. Biol. Chem.* **269**, 19183–19191.
10. Sechler, J. L., Rao, H., Cumiskey, A. M., Vega-Colon, I., Smith, M. S., Murata, T. & Schwarzbauer, J. E. (2001). A novel fibronectin binding site required for fibronectin fibril growth during matrix assembly. *J. Cell. Biol.* **154**, 1081–1088.
11. Litvinovich, S. V. & Ingham, K. C. (1995). Interactions between type III domains in the 110 kDa cell-binding fragment of fibronectin. *J. Mol. Biol.* **248**, 611–626.
12. Spitzfaden, C., Grant, R. P., Mardon, H. J. & Campbell, I. D. (1997). Module–module interactions in the cell-binding region of fibronectin: stability, flexibility and specificity. *J. Mol. Biol.* **265**, 565–579.
13. Plaxco, K. W., Spitzfaden, C., Campbell, I. D. & Dobson, C. M. (1997). A comparison of the folding kinetics and thermodynamics of two homologous fibronectin type III modules. *J. Mol. Biol.* **270**, 763–770.
14. Cota, E. & Clarke, J. (2000). Folding of beta-sandwich proteins: three-state transition of a fibronectin type III module. *Protein Sci.* **9**, 112–120.
15. Paci, E. & Karplus, M. (1999). Forced unfolding of fibronectin type 3 modules: an analysis by biased molecular dynamics simulations. *J. Mol. Biol.* **288**, 441–459.
16. Paci, E. & Karplus, M. (2000). Unfolding proteins by external forces and temperature: the importance of topology and energetics. *Proc. Natl Acad. Sci. USA*, **97**, 6521–6526.
17. Krammer, A., Lu, H., Isralewitz, B., Schulten, K. & Vogel, V. (1999). Forced unfolding of the fibronectin type III module reveals a tensile molecular recognition switch. *Proc. Natl Acad. Sci. USA*, **96**, 1351–1356.
18. Craig, D., Krammer, A., Schulten, K. & Vogel, V. (2001). Comparison of the early stages of forced unfolding for fibronectin type III modules. *Proc. Natl Acad. Sci. USA*, **98**, 5590–5595.
19. Rief, M., Gautel, M., Oesterhelt, F., Fernandez, J. M. & Gaub, H. E. (1997). Reversible unfolding of individual titin immunoglobulin domains by AFM. *Science*, **276**, 1109–1112.
20. Rief, M., Gautel, M., Schemmel, A. & Gaub, H. E. (1998). The mechanical stability of immunoglobulin

and fibronectin III domains in the muscle protein titin measured by atomic force microscopy. *Biophys. J.* **75**, 3008–3014.

21. Rief, M., Pascual, J., Saraste, M. & Gaub, H. E. (1999). Single molecule force spectroscopy of spectrin repeats: low unfolding forces in helix bundles. *J. Mol. Biol.* **286**, 553–561.

22. Rief, M., Gautel, M. & Gaub, H. E. (2000). Unfolding forces of titin and fibronectin domains directly measured by AFM. *Advan. Expt. Med. Biol.* **481**, 129–136.

23. Oberhauser, A. F., Marszalek, P. E., Erickson, H. P. & Fernandez, J. M. (1998). The molecular elasticity of the extracellular matrix protein tenascin. *Nature*, **393**, 181–185.

24. Carrion-Vazquez, M., Oberhauser, A. F., Fowler, S. B., Marszalek, P. E., Broedel, S. E., Clarke, J. & Fernandez, J. M. (1999). Mechanical and chemical unfolding of a single protein: a comparison. *Proc. Natl Acad. Sci. USA*, **96**, 3694–3699.

25. Carrion-Vazquez, M., Oberhauser, A. F., Fisher, T. E., Marszalek, P. E., Li, H. & Fernandez, J. M. (2000). Mechanical design of proteins studied by single-molecule force spectroscopy and protein engineering. *Prog. Biophys. Mol. Biol.* **74**, 63–91.

26. Oberdoerfer, Y., Fuchs, H. & Janshoff, A. (2000). Conformational analysis of native fibronectin by means of force spectroscopy. *Langmuir*, **16**, 9955–9958.

27. Yang, G., Cecconi, C., Baase, W. A., Vetter, I. R., Breyer, W. A., Haack, J. A. *et al.* (2000). Solid-state synthesis and mechanical unfolding of polymers of T4 lysozyme. *Proc. Natl Acad. Sci. USA*, **97**, 139–144.

28. Oesterhelt, F., Oesterhelt, D., Pfeiffer, M., Engel, A., Gaub, H. E. & Muller, D. J. (2000). Unfolding pathways of individual bacteriorhodopsins. *Science*, **288**, 143–146.

29. Fisher, T. E., Carrion-Vazquez, M., Oberhauser, A. F., Li, H., Marszalek, P. E. & Fernandez, J. M. (2000). Single molecular force spectroscopy of modular proteins in the nervous system. *Neuron*, **27**, 435–446.

30. Best, R. B., Li, B., Steward, A., Daggett, V. & Clarke, J. (2001). Can non-mechanical proteins withstand force? Stretching barnase by atomic force microscopy and molecular dynamics simulation. *Biophys. J.* **81**, 2344–2356.

31. Furuike, S., Ito, T. & Yamazaki, M. (2001). Mechanical unfolding of single filamin A (ABP-280) molecules detected by atomic force microscopy. *FEBS Letters*, **498**, 72–75.

32. Watanabe, K., Nair, P., Labeit, D., Kellermayer, M., Greaser, M., Labeit, S. & Granzier, H. (2002). Molecular mechanics of cardiac titin's PEVK and N2B spring elements. *J. Biol. Chem.* **277**, 11549–11558.

33. Li, H., Oberhauser, A. F., Fowler, S. B., Clarke, J. & Fernandez, J. M. (2000). Atomic force microscopy reveals the mechanical design of a modular protein. *Proc. Natl Acad. Sci. USA*, **97**, 6527–6531.

34. Evans, E. & Ritchie, K. (1999). Strength of a weak bond connecting flexible polymer chains. *Biophys. J.* **76**, 2439–2447.

35. Zhang, B. & Evans, J. S. (2001). Modeling AFM-induced PEVK extension and the reversible unfolding of Ig/FNIII domains in single and multiple titin molecules. *Biophys. J.* **80**, 597–605.

36. Leahy, D. J., Aukhil, I. L. & Erickson, H. P. (1996). 2.0 Å crystal structure of a four-domain segment of human fibronectin encompassing the RGD loop and synergy region. *Cell*, **84**, 155–164.

37. Hamill, S. J., Meekhof, A. E. & Clarke, J. (1998). The effect of boundary selection on the stability and folding of the third fibronectin type III domain from human tenascin. *Biochemistry*, **37**, 8071–8079.

38. Potts, J. R., Bright, J. R., Bolton, D., Pickford, A. R. & Campbell, I. D. (1999). Solution structure of the N-terminal F1 module pair from human fibronectin. *Biochemistry*, **38**, 8304–8312.

39. Li, H., Oberhauser, A. F., Redick, S. D., Carrion-Vazquez, M., Erickson, H. P. & Fernandez, J. M. (2001). Multiple conformations of PEVK proteins detected by single-molecule techniques. *Proc. Natl Acad. Sci. USA*, **98**, 10682–10686.

40. Marko, J. F. & Siggia, E. D. (1995). Stretching DNA. *Macromolecules*, **28**, 8759–8770.

41. Li, H., Carrion-Vazquez, M., Oberhauser, A. F., Marszalek, P. E. & Fernandez, J. M. (2000). Point mutations alter the mechanical stability of immunoglobulin modules. *Nature Struct. Biol.* **7**, 1117–1120.

42. Politou, A. S., Gautel, M., Improta, S., Vangelista, L. & Pastore, A. (1996). The elastic I-band region of titin is assembled in a "modular" fashion by weakly interacting Ig-like domains. *J. Mol. Biol.* **255**, 604–616.

43. Bell, G. I. (1978). Models for the specific adhesion of cells to cells. *Science*, **200**, 618–627.

44. Merkel, R., Nassoy, P., Leung, A., Ritchie, K. & Evans, E. (1999). Energy landscapes of receptor-ligand bonds explored with dynamic force spectroscopy. *Nature*, **397**, 50–53.

45. Erickson, H. P., Carrell, N. & McDonagh, J. (1981). Fibronectin molecule visualized in electron microscopy: a long, thin, flexible strand. *J. Cell. Biol.* **91**, 673–678.

46. Galbraith, C. G. & Sheetz, M. P. (1999). Keratocytes pull with similar forces on their dorsal and ventral surfaces. *J. Cell. Biol.* **147**, 1313–1324.

47. Burton, K., Park, J. H. & Taylor, D. L. (1999). Keratocytes generate traction forces in two phases. *Mol. Biol. Cell.* **10**, 3745–3769.

48. Balaban, N. Q., Schwarz, U. S., Riveline, D., Goichberg, P., Tzur, G., Sabanay, I. *et al.* (2001). Force and focal adhesion assembly: a close relationship studied using elastic micropatterned substrates. *Nature Cell. Biol.* **3**, 466–472.

49. Ohashi, T., Kiehart, D. P. & Erickson, H. P. (1999). Dynamics and elasticity of the fibronectin matrix in living cell culture visualized by fibronectin-green fluorescent. *Proc. Natl Acad. Sci. USA*, **96**, 2153–2158.

50. Baneyx, G., Baugh, L. & Vogel, V. (2001). Coexisting conformations of fibronectin in cell culture imaged using fluorescence resonance energy transfer. *Proc. Natl Acad. Sci. USA*, **98**, 14464–14468.

51. Alon, R., Hammer, D. A. & Springer, T. A. (1995). Lifetime of the P-selectin-carbohydrate bond and its response to tensile force in hydrodynamic flow. *Nature*, **374**, 539–542.

52. Alon, R., Chen, S., Fuhlbrigge, R., Puri, K. D. & Springer, T. A. (1998). The kinetics and shear threshold of transient and rolling interactions of L-selectin with its ligand on leukocytes. *Proc. Natl Acad. Sci. USA*, **95**, 11631–11636.

53. Vogel, V., Thomas, W. E., Craig, D. W., Krammer, A. & Baneyx, G. (2001). Structural insights into the mechanical regulation of molecular recognition sites. *Trends Biotechnol.* **19**, 416–423.

54. Erickson, H. P. (1994). Reversible unfolding of fibronectin type III and immunoglobulin domains provides the structural basis for stretch and elasticity

of titin and fibronectin. *Proc. Natl Acad. Sci. USA*, **91**, 10114–10118.

55. Florin, E. L., Rief, M., Lehmann, H., Ludwig, M., Dornmair, C., Moy, V. T. & Gaub, H. E. (1995). Sensing specific molecular-interactions with the atomic force microscope. *Biosen. Bioelectr.* **10**, 895–901.

56. Hutter, J. L. & Bechhoffer, J. (1993). Calibration of atomic-force microscope tips. *Rev. Sci. Instrum.* **64**, 1868–1873.